The Effects of Climate Change on Tradeoffs Among Forest Ecosystem Services

Nicholas D. C. Kullman

A thesis
submitted in partial fulfillment of the
requirements for the degree of

Master of Science

University of Washington

2016

Committee:

Sándor F. Tóth, Chair

David Butman

W. Art Chaovalitwongse

Program Authorized to Offer Degree:
Quantitative Ecology and Resource Management

University of Washington

Abstract

The Effects of Climate Change on
Tradeoffs Among Forest Ecosystem Services

Nicholas D. C. Kullman

Chair of the Supervisory Committee:
Associate Professor Sándor F. Tóth
School of Environmental and Forest Sciences

DRAFT

Forests provide a bounty to humans through ecosystem services such as wildlife habitat, recreation, and water and air purification. Forest managers seek to maximize the provision of ecosystem services and often do so for multiple ecosystem services simultaneously. While many studies predict that climate change will impact forests' ability to provide ecosystem services, no research has addressed the question of how climate change will impact the joint provision of ecosystem services. I address this question here in an attempt to better understand how the relationships between ecosystem services will change with climate - for example, how much additional fire hazard must be assumed in order to maintain an amount of habitat for a particular species. To study this question, I consider the evolution of a forested area in the Deschutes National Forest under three climate scenarios of varying intensity. This area provides three competing ecosystem services whose joint provision is assessed under each of the climate scenarios: northern spotted owl habitat, water quality, and resistance to wildfire.

I find that . . .

TABLE OF CONTENTS

LIST OF FIGURES

LIST OF TABLES

GLOSSARY

CLIMATE PROJECTION: The IPCC defines a climate projection as a model-derived estimate of future climate. *See* CLIMATE SCENARIO[50].

CLIMATE SCENARIO: The IPCC defines a scenario as a coherent, internally consistent and plausible description of a possible future state of the world. Herein, I use this term synonymously with CLIMATE PROJECTION, since climate projections often underlie climate scenarios [50].

CLUSTER: Here, a set of contiguous forest stands whose combined area exceeds 200 ha

ECOSYSTEM SERVICE: Benefits that people receive from ecosystems, divided into four categories: supporting, provisioning, regulating and cultural [5]. Examples include food, soil formation, water purification, carbon storage, recreation, and education.

PARETO EFFICIENT: A solution to a multi-objective mathematical program is said to be Pareto efficient if no component of the solution can be improved without compromising at least one other component.

STAND DENSITY INDEX (SDI): Reineke's Stand Density Index is a measure of the stocking of a forest stand. See [53].

TRADEOFF: The sacrifice of achievement in one objective in order to achieve more in another.

ACKNOWLEDGMENTS

DRAFT

Thank you to all who contributed to my earning this degree.

DEDICATION

DRAFT

To ma femme and my family

Chapter 1

ASSESSING CHANGES IN TRADEOFFS AMONG ECOSYSTEM SERVICES IN THE DESCHUTES NATIONAL FOREST

1.1 Introduction

Forests play an important role in global ecological, social, and economic processes. They provide ecosystem services such as carbon storage, purification of water and air, wildlife habitat, recreation opportunities, and generate raw materials for goods such as food and lumber [18]. In managed forests, the extent to which forests provide these services depends in part on management practices. Optimal forest management seeks to ensure the sustained provision of these ecosystem services [1].

Like other ecosystems, forests will undergo changes as a result of the changing climate. Researchers anticipate new spatial distributions of tree species [36], increased sediment delivery to streams [31], and increasing disturbance regimes such as wildfires, drought, and insect infestation [67]. As this transformation occurs, forests' ability to provide ecosystem services will change. Increased frequency of disturbance regimes will impact forests' ability to store carbon [7] and provide wildlife habitat [46]. Water supplies that rely on forests' filtration capabilities may be impacted by the rising sediment levels predicted by Goode *et al.* [31].

Forest managers might need to consider the effects of the changing climate, because the time scale of forest development is of the same order as that on which climate change is predicted to operate [34]. Optimal forest management will likely differ under alternative future climates [41]. Decisions that would once have resulted in optimal achievement of ecosystem services, now under different climatic conditions, may no longer do so. Without consideration of climate change, forest management plans may restrict forests' potential to provide ecosystem services most effectively.

Many studies have addressed the impacts of climate change on forest ecosystem services in isolation[67][7][46]. However, because forests provide these ecosystem services in concert with one another (see, for example, Tóth and McDill [65]), it is necessary to also understand how climate impacts the relationships among them. Ecosystem services exist in either "bundles" or "stacks". Stacked ecosystem services are those that are not in conflict, such as the provision of old growth forest and northern spotted owl habitat. An improvement in one ecosystem service also improves the others in the stack. In contrast, bundled ecosystem services conflict with one another. Joint provision of bundled ecosystem services requires tradeoffs in one service in order to achieve more of another. Timber revenues and wildlife habitat provide an example of bundled ecosystem services.

Here, I consider the case of bundled ecosystem services and analyze how climate change impacts the tradeoff relationships among the ecosystem services in the bundle. Consider, for example, a forest planner who must sacrifice old growth forest in order to maintain a certain level of wildfire hazard. Does sacrificing the same amount of old growth forest yield the same decrease in fire hazard under different climate conditions? I posit that a better understanding of how climate change will impact tradeoffs among bundled ecosystem services will allow forest planners to make more informed management decisions.

1.2 Methods

In response to stakeholder and public wants, forest planners often manage forests for multiple ecosystem services, such as wildlife habitat, recreation, goods production, aesthetics, and carbon sequestration. Such ecosystem services are commonly in conflict with one another, meaning that a forest planner cannot simultaneously maximize the provision of all ecosystem services. Instead, provision of some services must be sacrificed to enable achievement in others. Best compromises must be sought among bundled ecosystem services.

The Drink Planning Area in the Deschutes National Forest is one example of a region in which forest planners must consider the tradeoffs among ecosystem services when making management decisions.

1.2.1 *Study system*

The study system for this analysis is the Drink Planning Area. The Drink is a 7056 ha area on the east slopes of the Cascade Mountain Range in the Deschutes National Forest (see Figure 1.1). Of the ecosystem services provided by the Drink, the US Forest Service has selected three for prioritization.

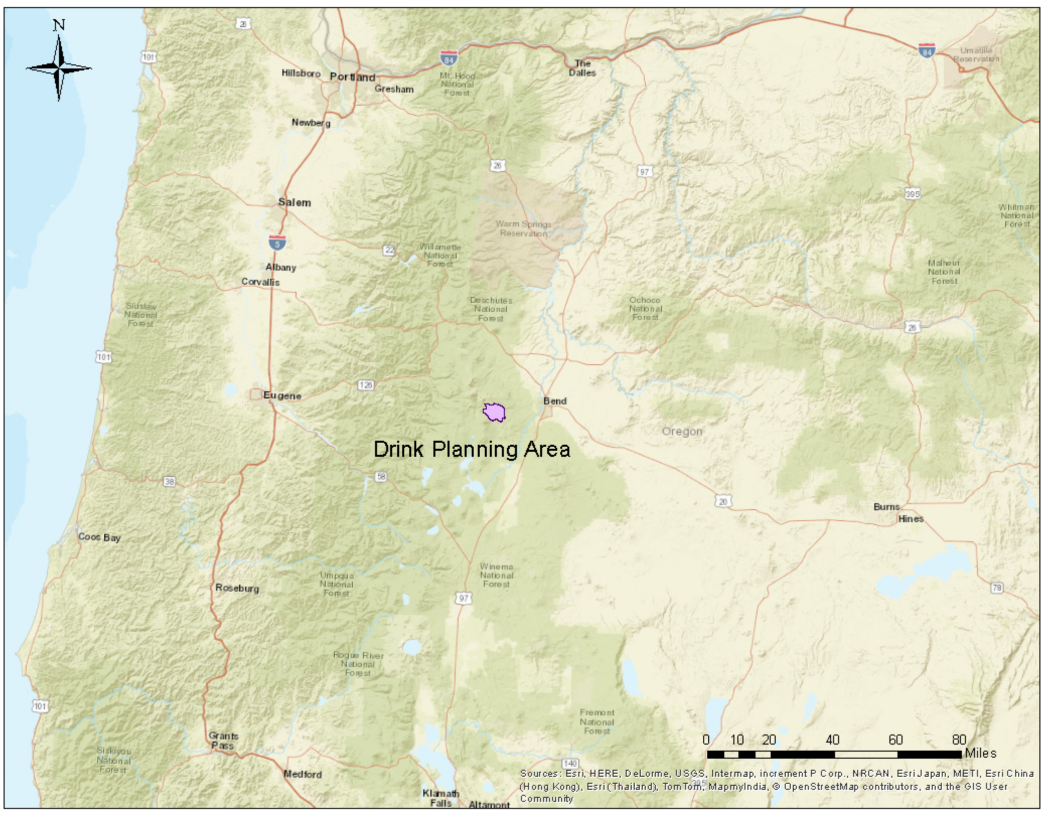

Figure 1.1: Overview of the study system, the Drink Planning Area (in purple), consisting of 7056 ha in the Deschutes National Forest.

The first is the protection of the northern spotted owl (NSO) (*Strix occidentalis caurina*), a common, if controversial, indicator species in Pacific Northwest forests. Approximately 43% of the Drink serves as habitat for the NSO (see Figure 1.2), and the USFS must protect this

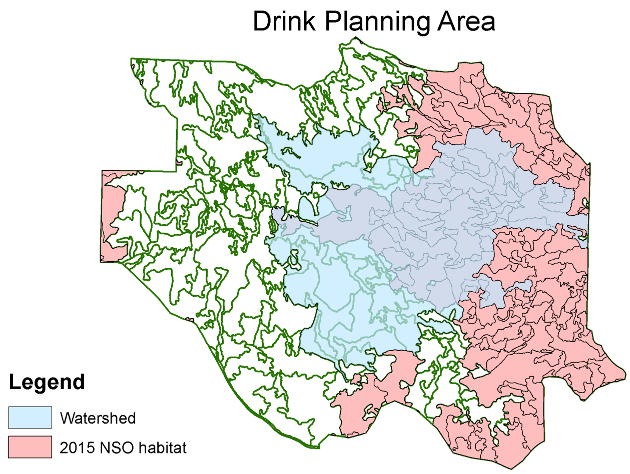

Figure 1.2: Location of the municipal watershed and the suitable NSO habitat in the Drink area at the beginning of the planning horizon (2015). Interior polygons are the 303 management units.

species since it is listed as threatened and therefore protected by the Endangered Species Act of 1973 [11].

The second objective is the reduction of the fire hazard rating across the Drink Area. Implementing silvicultural treatments to reduce the fire hazard of the Drink is critical because, in addition to providing NSO habitat, the municipal watershed for the cities of Bend, OR and Sisters, OR lies within the Drink (see Figure 1.2). These two cities have a combined population of approximately 90,000 people. Wildfires pose a threat to the their water supply, because wildfires cause soil water repellency, surface runoff, and debris torrents [35].

While the silvicultural treatments intend to provide long-term protection of the watershed, they also have the potential to introduce short-term increases in sediment delivery to the watershed [49]. The minimization of these short-term peaks in sediment delivery is the the final ecosystem service prioritized by the USFS.

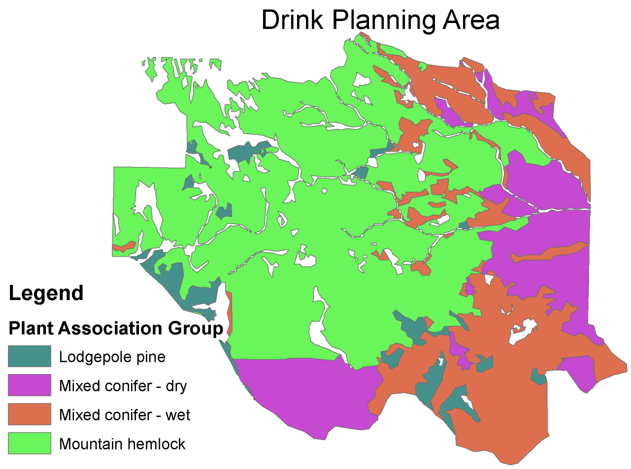

Figure 1.3: Plant association groups in the Drink Planning Area that were selected for potential treatments. Other plant association groups exist in the area but were not considered for treatment.

1.2.2 Timeline and assessment of treatment efficacy

Temporally, the case study in the Drink Planning Area consists of an 80 year simulation (2015 - 2095). All silvicultural treatments are performed in the first 40 years (2015 - 2055), divided into two 20-year planning periods. Spatially, the Drink is divided into 303 forest stands. Each stand may be treated in either period, neither, or both. Determining which treatment type to apply to a stand was done *a priori* and is entirely dependent on silvicultural characteristics; the rules governing this assignment of treatment type can be found in the appendix, §B.

To assess the treatments' long-term efficacy, the fire hazard rating of the Drink is measured at the end of the 80-year planning horizon in year 2095. The area of NSO habitat is assessed at the end of each planning period, years 2035 and 2055, to ensure that the application of treatments does not negatively impact the available habitat. Finally, at the time of treatment, the resulting short-term spikes in sediment delivery are measured. The time of treatment is assumed to be at the midpoint year in the planning period, years 2025 and 2045. A schematic of the planning horizon including the time of these events is shown in

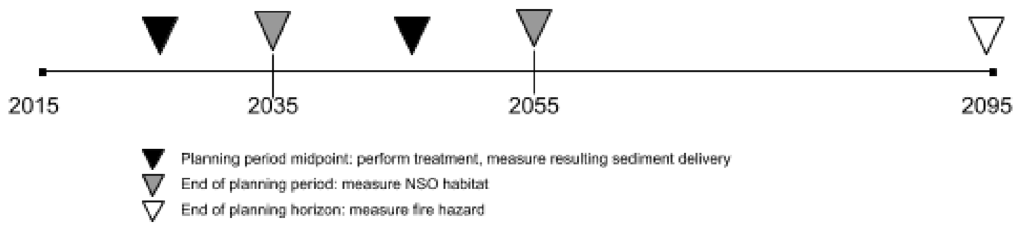

Figure 1.4: The planning horizon used in the analysis spans the 80 year period from 2015 to 2095. Treatments may be performed in the first period, the second period, both, or neither. Treatments are assumed to be performed at the mid-point years of each period (black triangles). Sediment delivery is measured on treatment years. Stands' suitability for NSO habitat is measured at the end of the planning periods (gray triangles), and stands' fire hazard ratings are measured at the end of the planning horizon (white triangle).

Figure 1.4.

Competition exists between these bundled ecosystem services: fuel treatments in the watershed drive short-term peaks in sediment delivery and have the potential to reduce owl habitat; yet the prioritization of either NSO habitat or water quality alone entails fewer fuel treatments and increased fire hazard rating as a result. The forest planner, here the USFS, seeks a management plan that balances the provision of these bundled ecosystem services. The ability of the forest planer to decide on such a plan may be improved given a better understanding of the tradeoff relationships among the ecosystem services in the bundle. In this study, I seek to provide information on these tradeoff relationships and do so in a novel approach that also considers the impacts on climate change.

1.2.3 Climate Scenarios Considered

The IPCC uses a scenario-based approach to predicting climate change, presenting many models of future climates from research agencies around the world. There is no attempt to predict which future climate is most likely or quantify the probability of realization of any one scenario. I employ the same approach here in studying the potential impacts of climate change on tradeoff relationships among bundled ecosystem services. For a set of future climate scenarios, the joint provision of a bundle of ecosystem services is assessed.

The alternative future climates considered in this study are climate scenarios from the first working group (WG1) of the IPCC's Fifth Assessment (AR5) [34]. Given the large number of potential future climates considered by the IPCC (see the list of experiments considered in AR5 [23]) combined with the computational complexity involved in the study of each one, I selected a small subset of three future climate scenarios for this analysis. Hereafter the scenarios are referred to as "None", "Ensemble RCP 4.5", and "Ensemble RCP 8.5".

The first scenario, "None", is the assumption of no climate change. While the number of studies incorporating climate change is increasing, this is still the assumption used for many modern studies such as Schroder (2013) [56], from which this study is derived. Because it has served as the basis for many studies and assumes a static environment resembling today's, the "None" climate scenario serves as a good control against which to compare the other two future climate scenarios.

As their names suggest, the second and third scenarios are ensembles. Each ensemble is an assembly of 17 global circulation models (GCMs) used in IPCC AR5. The selection of component GCMs in the ensembles was performed by the USFS's Climate-FVS [22] team. The list of the 17 scenarios included in the ensemble can be found in Crookston (2016) [14]. Each component GCM has a corresponding climate surface which contains a vector of 35 climate parameters at over 11,000 global locations for three time periods. The climate surfaces for the ensembles were created by averaging the values of all component GCMs for each climate parameter and each time period for each location. The result is a climate surface that, while temporally sparse, is spatially robust. Such a configuration is suited for use in the Drink area given the area's variance in elevation and slow vegetation growth.

The two ensembles are comprised of the same 17 GCMs, but the assumed representative concentration pathways (RCP) in the component GCMs differ. The RCP indicates the additional radiative forcing in W/m^2 above pre-industrial levels, with higher values of forcing indicative of more severe climate change. The GCMs in the Ensemble RCP 4.5 scenario assume 4.5 W/m^2 of additional radiative forcing, and the GCMs in the Ensemble RCP 8.5 scenario assume 8.5 W/m^2 of additional radiative forcing.

These three scenarios were chosen for the analysis as they represent a range of predicted climate change severity, from a 0°C warming by the year 2100 under the "None" scenario to a $2.6-4.8$°C warming under RCP 8.5 [34].

1.2.4 Determining tradeoff relationships between ecosystem services and climate scenarios

Each climate scenario is used to parameterize a multi-objective mathematical optimization model. These models determine the allocation of resources for optimal achievement of the objectives. Here, the resources are the application of fuel treatments and the objectives are the ecosystem services prioritized by the Forest Service: NSO habitat, fire hazard reduction, and short-term sediment delivery.

Solving each model generates a suite of management alternatives providing varying amounts in each ecosystem service. Comparing the ecosystem service achievements across the management alternatives reveals the tradeoff relationships among the ecosystem services. Since each model is parameterized according to a particular climate scenario, comparing the tradeoff relationships across models reveals how climate change impacts these tradeoffs among ecosystem services.

1.2.5 The Multi-objective Optimization Model

This section describes the multi-objective zero-one mathematical program to optimize the joint provision of ecosystem services in the Drink area. The model minimizes the fire hazard rating of the area, minimizes the peak sediment delivery occurring as a result of performing fuel treatments, and maximizes the minimum area of NSO habitat after treatment periods in the planning horizon.

Notation

The following notation is used in the model:

Parameters

- $i \in I$**:** the set of all 303 stands in the Drink area
- $r \in R$**:** the set of treatment schedule prescriptions:

$$r = \begin{cases} 1 & \text{treatment applied in the first period (2015-2035)} \\ 2 & \text{treatment applied in the second period (2035-2055)} \\ 3 & \text{treatment applied in both periods} \\ 0 & \text{no treatment applied in either period} \end{cases}$$

- $F_{i,r}$**:** the area-weighted fire hazard rating of stand i at the end of the planning horizon if prescribed to treatment schedule r
- $I_{\omega,t}$**:** the set of stands that can qualify as NSO habitat at the end of planning period t
- a_i**:** the area of stand i
- e**:** the discount factor applied to NSO habitat that is less than 200 ha in size
- $j \in R_{i,t}$**:** the set of treatment schedules such that stand i qualifies as NSO habitat in planning period t
- $s_{i,t}$**:** the contribution in tons of sediment delivered from performing fuel treatments on stand i in planning period t
- $c \in C$**:** the set of all clusters of stands whose combined area exceeds 200 hectares
- $i \in D_c$**:** the set of all stands that comprise cluster c

- $c \in C_i$**:** the set of all clusters that contain stand i

- A**:** the maximum area in hectares that may be treated in either planning period

- ℓ**,** u**:** the upper and lower bounds, respectively, on the relative fluctuation in the area treated in periods 1 and 2

Decision Variables

$$x_{i,r} = \begin{cases} 1 & \text{if stand } i \text{ is prescribed to treatment schedule } r \\ 0 & \text{otherwise} \end{cases}$$

Indicator Variables

- $q_{c,t} = 1$ if all stands in cluster c qualify as NSO habitat in planning period t and $q_{c,t} = 0$ otherwise

- $p_{i,t} = 1$ if in planning period t stand i is part of a cluster c such that $q_{c,t} = 1$; $p_{i,t} = 0$ otherwise

Accounting Variables

- S_t**:** the contribution in tons of sediment delivered from performing fuel treatments in planning period t

- O_t**:** the amount of NSO habitat in hectares at the end of planning period t

- H_t**:** the area in hectares treated in planning period t

Parameterization

The model was parameterized as follows:

- $F_{i,r}$: the metric for fire hazard rating used in this analysis originated in the work by Schroder *et al.* [56]. This metric was developed for the Drink area. It combines fire characteristics from Anderson's fuel models [4] to assign a fire hazard rating. I expanded the rating system to include fuel models not present in Schroder *et al.* See Table 1.1.

  The stands' fuels and vegetation characteristics to determine the fire hazard rating were generated using the US Forest Service's Climate-Forest Vegetation Simulator (FVS). Input vegetation data to Climate-FVS came from the 2012 GNN structure map (`http://lemma.forestry.oregonstate.edu/data/structure-maps`) from Oregon State University's Landscape Ecology, Modeling, Mapping & Analysis (LEMMA) group. Plots from the LEMMA database were mapped to the stands in the Drink area in order to produce tree and stand lists. These lists were used with Climate-FVS to simulate the stands' vegetation and fuels characteristics forward for the duration of the planning horizon under each climate scenario. Input climate data for Climate-FVS was obtained through the Climate-FVS climate data server [15].

- $I_{\omega,t}$: the set of stands that qualify as NSO habitat at the end of a planning period t are those that meet the following three criteria, as specified by the USFS:

  1. elevation less than 1830 m
  2. the presence of trees with DBH no less than 76 cm
  3. canopy closure of at least 60%

  The elevation requirement was checked using a digital elevation model from the US Department of Agriculture's GeoSpatial Data Gateway; canopy closure and large tree requirements were determined using the simulated vegetation characteristics output from Climate-FVS.

  To account for the NSO's large habitat requirements, stands must also be members of a cluster exceeding 200 ha in size, all of which meet the above three NSO habitat criteria. Stands not part of such a cluster have their contributions to owl habitat discounted by a factor of e.

- **e:** the discount factor for sub-200 ha NSO habitat was set to $e = 0.5$ following the convention used in Schroder *et al.* [56].

- **$j \in R_{i,t}$:** each stand-treatment schedule combination is evaluated at the end of each planning period to determine its suitability as NSO habitat. Treatment schedules for which stand i meets the criteria described above become members of the set $R_{i,t}$.

- **$s_{i,t}$:** the contributions of sediment delivery were determined using the Watershed Erosion Prediction Project (WEPP) online GIS tool [28]. This tool takes as input soil textures, treatment types, duration of simulation, and custom climate data. I obtained soil texture data for the Drink area from the USDA's Soil Survey Geographic (SSURGO) database. Treatment types are those specified in §B, and the years of simulation correspond to the treatment years in the model's planning horizon. The custom climate data are the same data described above for use with Climate-FVS, obtained through the Climate-FVS data server.

- **A:** the maximum area that may be treated in either planning period was defined to be 6000 acres, or approximately 2428 ha

- **ℓ, u:** the relative fluctuation in the area treated in periods 1 and 2 was defined to be 20%. That is, $\ell = 0.8$ and $u = 1.2$.

Formulation

The formulation of the model is as follows:

Fuel Model	**Fire Hazard Rating**	Group	Flame length (m)	Rate of spread (m/hr)	Total fuel load (tons/ha)
4*	**5**	Shrub	5.79	1508.76	32.12
5	**4**	Shrub	1.22	362.10	8.65
8	**1**	Timber	0.30	32.19	12.36
9*	**2**	Timber	0.79	150.88	8.65
10	**2**	Timber	1.46	158.92	29.65
11*	**2**	Logging Slash	1.07	120.7	28.42
12	**4**	Logging Slash	2.44	261.52	85.50
13	**5**	Logging Slash	3.20	271.58	143.57

Table 1.1: Fire hazard rating system used here, originally employed by Schroder *et al.* [56].
* denotes fuel models not present in Schroder *et al.*
The fuel model column refers to the Anderson fuel model ratings [4].

Minimize

$$\sum_{i \in I} \sum_{r \in R} F_{i,r} x_{i,r} \tag{1.1}$$

$$\max\{S_1, S_2\} \tag{1.2}$$

Maximize

$$\min\{O_1, O_2\} \tag{1.3}$$

Subject to:

$$\sum_{i\in I_{\omega,t}}\left(a_i p_{i,t} + e a_i \left(\sum_{j\in R_{i,t}} x_{i,j} - p_{i,t}\right)\right) = O_t \qquad \forall t \in \{1,2\} \tag{1.4}$$

$$\sum_{i\in I}\sum_{r\in 1,3} s_{i,1}x_{i,r} = S_1 \tag{1.5}$$

$$\sum_{i\in I}\sum_{r\in 2,3} s_{i,2}x_{i,r} = S_2 \tag{1.6}$$

$$\sum_{i\in D_c}\sum_{j\in R_{i,t}} x_{i,j} - |c|q_{c,t} \geq 0 \qquad \forall t \in \{1,2\}, c \in C \tag{1.7}$$

$$\sum_{c\in C_i} q_{c,t} - p_{i,t} \geq 0 \qquad \forall t \in \{1,2\}, i \in I_{\omega,t} \tag{1.8}$$

$$\sum_{r\in R} x_{i,r} = 1 \qquad \forall i \in I \tag{1.9}$$

$$\sum_{i\in I}\sum_{r\in 1,3} a_i x_{i,r} = H_1 \tag{1.10}$$

$$\sum_{i\in I}\sum_{r\in 2,3} a_i x_{i,r} = H_2 \tag{1.11}$$

$$H_t \leq A \qquad \forall t \in \{1,2\} \tag{1.12}$$

$$\ell H_1 - H_2 \leq 0 \tag{1.13}$$

$$-uH_1 + H_2 \leq 0 \tag{1.14}$$

$$x_{i,r}, p_i, q_c \in \{0,1\} \quad \forall i \in I, r \in R, c \in C \tag{1.15}$$

Equations (1.1)-(1.3) are the objective functions: equation (1.1) minimizes the cumulative fire hazard rating of the Drink area at the end of the 80-year planning horizon, equation (1.2) minimizes the maximum peak in sediment delivery for the two planning periods, and equation (1.3) maximizes the minimum NSO habitat available at the end of the planning periods. Equation set (1.4) defines the amount of NSO habitat available at the end of the planning horizons. Note that if stand i does not belong to a cluster of NSO habitat exceeding 200 hectares, then its area contribution to total NSO habitat is discounted by a factor of e. Equations (1.5) and (1.6) define the sediment delivered in planning periods one and two, respectively.

Inequality set (1.7) controls the value of the cluster variables $q_{c,t}$ indicating clusters of suitable NSO habitat in each of the planning periods. Inequality set (1.8) controls the value of the $p_{i,t}$ variables indicating stands' inclusion in NSO habitat clusters.

The set of equalities (1.9) enforces the logical constraint that each stand must be prescribed to exactly one treatment schedule. Equations (1.10) and (1.11) are accounting constraints for the total area treated in each planning period, and inequalities (1.12) ensure that this area does not exceed the predefined per-period maximum. Inequalities (1.13) and (1.14) bound the fluctuation in treated area between the planning periods. Finally, constraint (1.15) defines the decision and indicator variables as binary.

1.2.6 Model Solution and Comparing Efficient Frontiers

I wrote an implementation of Tóth's Alpha-Delta algorithm [62] to solve the models utilizing the IBM ILOG CPLEX optimization engine. For a problem with N objectives, the Alpha-Delta algorithm finds the optimal set of solutions by iteratively slicing the N-dimensional objective space with a tilted $N-1$ dimensional plane. The algorithm was implemented using an alpha parameter of $\alpha = .01$ and delta parameters of $\delta_{Hab} = 1$ ha and $\delta_{Sed} = 2$ tons for the NSO habitat and sediment delivery objectives, respectively.

Solving a bounded and non-degenerate multi-objective optimization problem with N objectives produces a set of objective vectors (also called "solutions") $\mathbf{z} \in Z$ where $\mathbf{z} = \langle z^1, \ldots, z^N \rangle$. The set of solutions Z is referred to as the Pareto-optimal frontier or efficient frontier or, simply, frontier. The solutions comprising an efficient frontier have the special relationship such that no component of a solution $\mathbf{z}^i$ can be improved upon without one of the other components $\mathbf{z}^j$ $(j \neq i)$ degrading. This quality is known as Pareto efficiency. For example, this relationship in the current problem means that further reducing the value of fire hazard in a solution would result in either additional sediment delivery, a reduction of NSO habitat, or both.

Thus the efficient frontier provides information on the tradeoff relationship that exists between ecosystem services. Parameterizing and solving the above model for each of the climate scenarios generates three frontiers: Z_{None}, $Z_{4.5}$, and $Z_{8.5}$ for the None, Ensemble RCP 4.5, and Ensemble RCP 8.5 scenarios, respectively. Since climate data alone differentiates the models and their resulting frontiers, comparing the frontiers reveals how climate impacts the tradeoff relationships among the ecosystem services. However, no standardized procedure exists to compare frontiers.

One applicable metric is the volume of the N-dimensional objective space bounded by the frontier, known as the hypervolume indicator. With Sándor Tóth, I devised an algorithm to compute the value of the hypervolume indicator for a frontier. The algorithm proceeds by sorting the solutions according to one objective, then iteratively adds them to the frontier, each time computing the additional volume enclosed by the solution. Details of the algorithm may be found in the appendix, §A.

We developed this algorithm independently but later discovered that researchers in the field of Evolutionary Multiobjective Optimization (EMO) have developed their own algorithms to compute the hypervolume indicator. In the present study, the metric is used to compute the impact of climate change on tradeoff relationships among ecosystem services; in EMO, the metric is commonly used to assess the quality of algorithms used in heuristic searches of Pareto frontiers. Hence, while the metric is the same, the algorithm to compute it and its application are unique in this study.

Upon realization of the use of the hypervolume indicator in EMO, I discovered additional frontier comparison methods used in this field and adopted them for use here. These methods include the additive binary epsilon and binary hypervolume indicators, and the unary distance, additive unary epsilon, and unary spacing indicators. Information on these metrics can be found in the appendix, §C.1.

In addition to frontier-level comparisons, it is also worthwhile to consider how climate change may impact the relationship between two specific ecosystem services within the frontier. Here, I use two methods to determine this: 1) the hypervolume indicator of the nondominated frontier points in the projection, and 2) the Pearson correlation coefficient between all points on the frontier. Details on these methods may be found in the appendix, §C.2.

1.3 Results and Discussion

DRAFT

The frontiers for each climate scenario can be found in Figure ...

1.4 Conclusion

DRAFT

I find that climate change has positive impacts on the tradeoff structure between managed ecosystem services in the Drink Area ...

BIBLIOGRAPHY

[1] 36 CFR 219.1. National forest system land management planning, 2012.

[2] Fouad Ben Abdelaziz. Solution approaches for the multiobjective stochastic programming. *European Journal of Operational Research*, 216(1):1–16, 2012.

[3] Frank A Albini. Estimating wildfire behavior and effects. 1976.

[4] Hal E Anderson. Aids to determining fuel models for estimating fire behavior. *The Bark Beetles, Fuels, and Fire Bibliography*, page 143, 1982.

[5] Millennium Ecosystem Assessment et al. *Ecosystems and human well-being*, volume 5. Island press Washington, DC:, 2005.

[6] Brad Bass, Guohe Huang, and Joe Russo. Incorporating climate change into risk assessment using grey mathematical programming. *Journal of Environmental Management*, 49(1):107 – 123, 1997.

[7] Gordon B Bonan. Forests and climate change: forcings, feedbacks, and the climate benefits of forests. *Science*, 320(5882):1444–1449, 2008.

[8] Jose G Borges, Jordi Garcia-Gonzalo, Vladimir Bushenkov, Marc E McDill, Susete Marques, and Manuela M Oliveira. Addressing multicriteria forest management with pareto frontier methods: An application in portugal. *Forest Science*, 60(1):63–72, 2014.

[9] Brett A. Bryan and Neville D. Crossman. Systematic regional planning for multiple objective natural resource management. *Journal of Environmental Management*, 88(4):1175 – 1189, 2008.

[10] Kai MA Chan, M Rebecca Shaw, David R Cameron, Emma C Underwood, and Gretchen C Daily. Conservation planning for ecosystem services. *PLoS biology*, 4(11):e379, 2006.

[11] US Congress. Endangered species act. *Washington DC*, 1973.

[12] Ira R. Cooke, Simon A. Queenborough, Elizabeth H. A. Mattison, Alison P. Bailey, Daniel L. Sandars, A. R. Graves, J. Morris, Philip W. Atkinson, Paul Trawick, Robert P. Freckleton, Andrew R. Watkinson, and William J. Sutherland. Integrating socio-economics and ecology: a taxonomy of quantitative methods and a review of their use in agro-ecology. *Journal of Applied Ecology*, 46(2):269–277, 2009.

[13] Steven P Courtney and Andrew B Carey. *Scientific evaluation of the status of the Northern Spotted Owl*. Sustainable Ecosystems Institute Portland, OR, 2004.

[14] Nicholas Crookston. Details of data and methods used for calculating future climate estimates, 2016.

[15] Nicholas Crookston. Get climate-fvs ready data, 2016.

[16] Nicholas L Crookston. Climate-fvs version 2: Content, users guide, applications, and behavior. 2014.

[17] Piotr Czyzżak and Adrezej Jaszkiewicz. Pareto simulated annealingâĂŤa metaheuristic technique for multiple-objective combinatorial optimization. *Journal of Multi-Criteria Decision Analysis*, 7(1):34–47, 1998.

[18] Gretchen C Daily, Susan Alexander, Paul R Ehrlich, Larry Goulder, Jane Lubchenco, Pamela A Matson, Harold A Mooney, Sandra Postel, Stephen H Schneider, David Tilman, et al. *Ecosystem services: benefits supplied to human societies by natural ecosystems*, volume 2. Ecological Society of America Washington (DC), 1997.

[19] Kalyanmoy Deb. *Multi-objective optimization using evolutionary algorithms*, volume 16. John Wiley & Sons, 2001.

[20] Kalyanmoy Deb and Dhish Kumar Saxena. On finding pareto-optimal solutions through dimensionality reduction for certain large-dimensional multi-objective optimization problems. *Kangal report*, 2005011, 2005.

[21] Luis Diaz-Balteiro and Carlos Romero. Making forestry decisions with multiple criteria: a review and an assessment. *Forest Ecology and Management*, 255(8):3222–3241, 2008.

[22] Gary E Dixon et al. Essential fvs: A userâĂŹs guide to the forest vegetation simulator. *Fort Collins, CO: USDA-Forest Service, Forest Management Service Center*, 2002.

[23] German Climate Computing Centre (DKRZ). IPCC working group i AR5 snapshot.

[24] Oregon Fish and Wildlife Office. Species fact sheet: Northern spotted owl. `http://www.fws.gov/oregonfwo/Species/Data/NorthernSpottedOwl/default.asp`. Accessed: 2015-02-06.

[25] US Fish, Wildlife Service, et al. Revised recovery plan for the northern spotted owl (strix occidentalis caurina). *USDI Fish and Wildlife Service, Portland, OR USA*, 2011.

[26] Forestières Internationaler Verband Forstlicher Forschungsanstalten. Adaptation of forests and people to climate change. 2009.

[27] Eclipse Foundation. Eclipse, 2014.

[28] James R Frankenberger, Shuhui Dun, Dennis C Flanagan, Joan Q Wu, and William J Elliot. Development of a gis interface for WEPP model application to great lakes forested watersheds. In *International Symposium on Erosion and Landscape Evolution (ISELE), 18-21 September 2011, Anchorage, Alaska*, page 139. American Society of Agricultural and Biological Engineers, 2011.

[29] William L Gaines, Richy J Harrod, James Dickinson, Andrea L Lyons, and Karl Halupka. Integration of northern spotted owl habitat and fuels treatments in the eastern cascades, washington, usa. *Forest Ecology and Management*, 260(11):2045–2052, 2010.

[30] J Garcia-Gonzalo, JG Borges, JHN Palma, and A Zubizarreta-Gerendiain. A decision support system for management planning of eucalyptus plantations facing climate change. *Annals of Forest Science*, 71(2):187–199, 2014.

[31] Jaime R. Goode, Charles H. Luce, and John M. Buffington. Enhanced sediment delivery in a changing climate in semi-arid mountain basins: Implications for water resource management and aquatic habitat in the northern rocky mountains. *Geomorphology*, 139âĂŞ140(0):1 – 15, 2012.

[32] Lee E Harding and Emily McCullum. Ecosystem response to climate change in british columbia and yukon: threats and opportunities for biodiversity. *Responding to global climate change in British Columbia and Yukon*, 1:9–1, 1997.

[33] Grant Hauer, Steve Cumming, Fiona Schmiegelow, Wiktor Adamowicz, Marian Weber, and Robert Jagodzinski. Tradeoffs between forestry resource and conservation values under alternate policy regimes: A spatial analysis of the western canadian boreal plains. *Ecological Modelling*, 221(21):2590 – 2603, 2010.

[34] IPCC Working Group I. *Climate Change 2013-The Physical Science Basis: Summary for Policymakers.* Intergovernmental Panel on Climate Change, 2013.

[35] George G Ice, Daniel G Neary, and Paul W Adams. Effects of wildfire on soils and watershed processes. *Journal of Forestry*, 102(6):16–20, 2004.

[36] Louis R Iverson and Anantha M Prasad. Predicting abundance of 80 tree species following climate change in the eastern united states. *Ecological Monographs*, 68(4):465–485, 1998.

[37] Amit Kanudia and Richard Loulou. Robust responses to climate change via stochastic markal: The case of quÃľbec. *European Journal of Operational Research*, 106(1):15 – 30, 1998.

[38] Vineet Khare, Xin Yao, and Kalyanmoy Deb. Performance scaling of multi-objective evolutionary algorithms. In *Evolutionary Multi-Criterion Optimization*, pages 376–390. Springer, 2003.

[39] Joshua Knowles and David Corne. On metrics for comparing nondominated sets. In *Evolutionary Computation, 2002. CEC'02. Proceedings of the 2002 Congress on*, volume 1, pages 711–716. IEEE, 2002.

[40] Danny C Lee and Larry L Irwin. Assessing risks to spotted owls from forest thinning in fire-adapted forests of the western united states. *Forest Ecology and Management*, 211(1):191–209, 2005.

[41] Marcus Linder. Developing adaptive forest management strategies to cope with climate change. *Tree Physiology*, 20(5-6):299–307, 2000.

[42] Alexander V Lotov, Vladimir A Bushenkov, and Georgy K Kamenev. *Interactive decision maps: Approximation and visualization of Pareto frontier*, volume 89. Springer, 2004.

[43] Alexander V Lotov and Kaisa Miettinen. Visualizing the pareto frontier. In *Multiobjective optimization*, pages 213–243. Springer, 2008.

[44] B Luo, I Maqsood, YY Yin, GH Huang, and SJ Cohen. Adaption to climate change through water trading under uncertainty- an inexact two-stage nonlinear programming approach. *Journal of Environmental Informatics*, 2(2):58–68, 2003.

[45] Shunsuke Managi. Evaluation and policy analysis of japanese forestry. In *2005 Annual meeting, July 24-27, Providence, RI*, number 19358. American Agricultural Economics Association (New Name 2008: Agricultural and Applied Economics Association), 2005.

[46] Donald McKenzie, Ze'ev Gedalof, David L Peterson, and Philip Mote. Climatic change, wildfire, and conservation. *Conservation Biology*, 18(4):890–902, 2004.

[47] Robin Naidoo, Andrew Balmford, Robert Costanza, Brendan Fisher, Rhys E Green, B Lehner, TR Malcolm, and Taylor H Ricketts. Global mapping of ecosystem services and conservation priorities. *Proceedings of the National Academy of Sciences*, 105(28):9495–9500, 2008.

[48] Craig R. Nitschke and John L. Innes. Integrating climate change into forest management in south-central british columbia: An assessment of landscape vulnerability and development of a climate-smart framework. 2008.

[49] Jay OâĂŹLaughlin. Conceptual model for comparative ecological risk assessment of wildfire effects on fish, with and without hazardous fuel treatment. *Forest Ecology and Management*, 211(1):59–72, 2005.

[50] Intergovernmental Panel on Climate Change. Definition of terms used within the DDC pages. `http://www.ipcc-data.org/guidelines/pages/definitions.html`, 2013.

[51] Intergovernmental Panel on Climate Change. Scenario Process for AR5. `http://sedac.ipcc-data.org/ddc/ar5\_scenario\_process/scenario\_background.html`, 2014.

[52] M. Pasalodos-Tato, A. MÃďkinen, J. Garcia-Gonzalo, J.G. Borges, T. LÃďmÃěs, and L.O. Eriksson. Review. assessing uncertainty and risk in forest planning and decision support systems: review of classical methods and introduction of new approaches. *Forest Systems*, 22(2), 2013.

[53] Lester Henry Reineke. Perfecting a stand-density index for even-aged forests. 1933.

[54] Elizabeth Reinhardt and Nicholas L Crookston. The fire and fuels extension to the forest vegetation simulator. 2003.

[55] Jason R Schott. Fault tolerant design using single and multicriteria genetic algorithm optimization. Technical report, DTIC Document, 1995.

[56] Svetlana A (Kushch) Schroder, Sándor F Tóth, Robert L Deal, and Ettl Gregory J. Multi-objective optimization to evaluate tradeoffs among forest ecosystem services following fire hazard reduction in the Deschutes National Forest, USA. *Ecosystem Services*, Special Issue "Integrated Valuation of Ecosystem Services: Challenges and Solutions", accepted.

[57] Svetlana Kushch Schroder. *Optimizing forest management in consideration of environmental regulations, economic constraints, and ecosystem services.* PhD thesis, 2013.

[58] Rupert Seidl, Werner Rammer, Dietmar Jäger, and Manfred J Lexer. Impact of bark beetle (< i> ips typographus</i> l.) disturbance on timber production and carbon sequestration in different management strategies under climate change. *Forest Ecology and Management*, 256(3):209–220, 2008.

[59] Daniel Simberloff. Flagships, umbrellas, and keystones: is single-species management passé in the landscape era? *Biological conservation*, 83(3):247–257, 1998.

[60] Soil Survey Staff. Soil survey geographic (ssurgo) database.

[61] Chris D Thomas, Alison Cameron, Rhys E Green, Michel Bakkenes, Linda J Beaumont, Yvonne C Collingham, Barend FN Erasmus, Marinez Ferreira De Siqueira, Alan Grainger, Lee Hannah, et al. Extinction risk from climate change. *Nature*, 427(6970):145–148, 2004.

[62] Sándor Tóth. *Modeling Timber and Non-timber Trade-offs in Spatially-Explicit Forest Planning.* PhD thesis.

[63] Sándor Tóth and Marc McDill. Finding efficient harvest schedules under three conflicting objectives. 2009.

[64] Sándor Tóth, Marc McDill, and Stephanie Rebain. Finding the efficient frontier of a bi-criteria, spatially explicit, harvest scheduling problem. 2006.

[65] Sándor F Tóth and Marc E McDill. Finding efficient harvest schedules under three conflicting objectives. *Forest Science*, 55(2):117–131, 2009.

[66] Fernando Badilla Veliz, Jean-Paul Watson, Andres Weintraub, Roger J-B Wets, and David L Woodruff. Stochastic optimization models in forest planning: a progressive hedging solution approach. *Annals of Operations Research*, pages 1–16, 2014.

[67] James M Vose, David Lawrence Peterson, Toral Patel-Weynand, et al. *Effects of climatic variability and change on forest ecosystems: a comprehensive science synthesis for the US forest sector.* US Department of Agriculture, Forest Service, Pacific Northwest Research Station Portland, OR, 2012.

[68] Andy White and Alejandra Martin. Who owns the worldâĂŹs forests. *Forest Trends, Washington, DC*, 2002.

[69] Steven M Wondzell and John G King. Postfire erosional processes in the pacific northwest and rocky mountain regions. *Forest Ecology and Management*, 178(1):75–87, 2003.

[70] Rasoul Yousefpour, Jette Bredahl Jacobsen, Bo Jellesmark Thorsen, Henrik Meilby, Marc Hanewinkel, and Karoline Oehler. A review of decision-making approaches to handle uncertainty and risk in adaptive forest management under climate change. *Annals of forest science*, 69(1):1–15, 2012.

[71] Eckart Zitzler. *Evolutionary algorithms for multiobjective optimization: Methods and applications*, volume 63. Citeseer, 1999.

[72] Eckart Zitzler, Lothar Thiele, Marco Laumanns, Carlos M Fonseca, and Viviane Grunert Da Fonseca. Performance assessment of multiobjective optimizers: an analysis and review. *Evolutionary Computation, IEEE Transactions on*, 7(2):117–132, 2003.

Appendix A
COMPUTING A FRONTIER'S HYPERVOLUME INDICATOR

Given a set of Pareto optimal solutions $\mathcal{P}$ to a multi-objective mathematical programming model with a set of objectives O of cardinality $N := |O|$, this algorithm computes the volume V of the objective space bounded by the Pareto frontier defined by the solutions $x \in \mathcal{P}$. The objectives are assumed to be normalized so that the objective space is the N-dimensional unit hypercube with the origin and the point $\vec{\mathbf{1}}$ defining the nadir objective vector and the ideal objective vector, respectively. That is, all objectives are assumed to be maximized with bounds $[0, 1]$.

The algorithm projects the objective space into $N - 1$ dimensions by eliminating the dimension associated with an (arbitrarily-chosen) objective $p \in O$. The set of objectives is $\overline{O} := O \backslash \{p\}$. It is assumed that $x \in \mathcal{P}$ are sorted in descending order according to p. The algorithm proceeds by sequentially adding solutions to the $(N - 1)$-dimensional space, and calculating the contribution to the frontier volume as a product of the volume contribution in $N - 1$ dimensions and its achievement in objective p.

Let $\overline{V_x}$ be the $(N - 1)$-dimensional volume contribution of solution x and x_p be the achievement of solution x in objective p. Further, let F be the set of non-dominated solutions in $N - 1$ dimensions. I compute the N-dimensional volume of the frontier V as follows.

Figure A.1: Algorithm to compute the unary hypervolume indicator of a Pareto frontier.

$V \leftarrow 0$
$\overline{V} \leftarrow 0$
$F \leftarrow \emptyset$
for all $x \in \mathcal{P}$ **do**
    $\overline{V}_x \leftarrow \prod_{o \in \overline{O}} x_o - \overline{V}$
    for all $f \in F$ **do**
        if $f_o < x_o \forall o \in \overline{O}$ **then**
            $F \leftarrow F \setminus \{f\}$
        end if
    end for
    for all $o \in \overline{O}$ **do**
        $F_{x,o} := \{\, f \in F : f_o > x_o \,\}$
        Sort $f \in F_{x,o}$ in ascending order by their oth component, f_o
        $v_i \leftarrow x_o$
        for all $f \in F_{x,o}$ **do**
            $v_t \leftarrow f_o$
            $\delta_o := v_t - v_i$
            $\overline{V}_x \leftarrow \overline{V}_x + \delta_o \prod_{\sigma \in \overline{O} \setminus \{o\}} f_\sigma$
            $v_i \leftarrow v_t$
        end for
    end for
    $F \leftarrow F \cup \{x\}$
    $\overline{V} \leftarrow \overline{V} + \overline{V}_x$
    $V \leftarrow V + x_p \overline{V}_x$
end for

Appendix B

TREATMENT SPECIFICATIONS FOR THE DRINK AREA

Vegetation conditions were assessed at the midpoint of each planning period. If a set of conditions as listed in Table B.1 were met, then the corresponding treatment was applied. Otherwise, no action was taken. Table adapted from Schroder [56].

Table B.1: Rules governing treatment assignments.

SDI[1]	**CBD**[2]	**TPH**$_{<18}$[3]	**Fuel model**[4]	**BA**$_{\mathrm{MHD+WF},>46}$[5]	**Treatment**
Lodgepole pine (LPD) plant association					
< 87	N/A	N/A	N/A	N/A	**Prescribed burn**
≥ 87	> 0.037	> 49	≥ 10	N/A	**Thin, pileburn slash and fuels**[6]
			< 10	N/A	**Thin, pileburn slash**
Mixed conifer wet (MCW) or mountain hemlock (MHD) plant associations					
< 87	N/A	N/A	N/A	N/A	**Prescribed burn**

[1] Stand Density Index, calculated in metric units (trees per ha).

[2] Crown bulk density (kg/m^3)

[3] Number of trees per hectare whose diameter at breast height (DBH) is less than 18 cm

[4] According to the Anderson rating system[4]

[5] Basal area in m^2 of all mountain hemlock (MHD) and white fir (WF) trees with DBH $> 46cm$.

[6] Pileburning slash involves removal of thinned trees only, while pileburning slash and fuels also involves removal of materials that were on the ground before thinning (Wall, Powers, 2012; personal communication)

≥ 87	> 0.037	> 49	$= 10$	> 7.5	**Thin, pileburn slash and fuels, prescribed burn**
				≤ 7.5	**Thin, pileburn slash and fuels**
			> 10	N/A	**Thin, pileburn slash and fuels**
			< 10	N/A	**Thin, pileburn slash**
		≤ 49	$= 10$	≥ 7.5	**Prescribed burn**
	≤ 0.037	N/A	$= 10$	≥ 7.5	**Prescribed burn**
	N/A	N/A	$\in \{6, 8, 9, 10\}$	N/A	**Prescribed burn**[7]
Mixed conifer dry (MCD) plant association					
< 87	N/A	N/A	N/A	N/A	**Prescribed burn**
≥ 87	> 0.037	> 49	$\in \{10, 11\}$	N/A	**Thin, pileburn slash and fuels, prescribed burn**
			≥ 12	N/A	**Thin, pileburn slash and fuels**
			< 10	N/A	**Thin, pileburn slash**
		≤ 49	$\in \{10, 11\}$	N/A	**Prescribed burn**
	≤ 0.037	N/A	$\in \{10, 11\}$	N/A	**Prescribed burn**
	N/A	N/A	$\in \{6, 8, 9, 10\}$	N/A	**Prescribed burn**[7]

[7] Only if prescribed burn was assigned in period 1 (applies to period 2 treatment assignments only)

Appendix C
INTER- AND INTRA-FRONTIER COMPARISON METRICS

This chapter describes in more detail the metrics used to compare the frontiers generated by solving the multi-objective model described in §1.2.5. The metrics are broken up into two groups. *Inter-frontier comparison metrics* are those metrics that quantify some feature of a frontier. That is, the metric has only a single value per frontier. These metrics may be used either alone or with other metrics to make comparisons at the frontier level. *Intra-frontier comparison metrics* are those metrics that quantify some feature within a frontier. There may be multiple values of this metric per frontier, depending on the metric and the number of objectives. These metrics may be used either alone or with other metrics to make comparisons at the objective (or ecosystem service) level.

C.1 Inter-Frontier Comparison Metrics

Researchers in the field of EMO develop algorithms to generate a set of non-dominated solutions that best represents the true Pareto-optimal frontier [19]. To test their algorithms, they solve a benchmark multi-objective optimization problem and compare their resulting frontiers to the known Pareto front for that problem [39]. There is no assurance of optimality of the solutions derived using these algorithms, so they require a means of comparing the resulting frontiers to determine if one algorithm produces a "better" non-dominated frontier than another. Zitzler et al. provide a review of comparison methods [72]. These methods aim to quantify certain traits about a frontier that can be used to measure their success in approximation of the true frontier.

When necessary, the normalization of the objective space is such that all objectives are maximized, and each frontier is contained within the unit hypercube. That is, each objective is bounded between 0 and 1, yielding a frontier bounded by $[0,1]^N$. Defining the nadir solution $\mathbf{z}_{\text{nad}}$ of a frontier of points $z \in Z$ as the objective vector with components

$$\mathbf{z}^i_{\text{nad}} = \inf_z \{z^i\} \quad \forall 1 \le i \le N \tag{C.1}$$

and the ideal solution as the objective vector with components

$$\mathbf{z}^i_{\text{ideal}} = \sup_z \{z^i\} \quad \forall 1 \le i \le N \tag{C.2}$$

then under my normalization, the nadir solution is the origin and the ideal solution is the N-dimensional vector of ones $\mathbf{1}_N$.

The definitions of dominance terms used here are in Table C.1.

Relation	**Solutions**		**Frontiers**	
Strictly dominates	$\mathbf{z}_1 \succ\succ \mathbf{z}_2$	$\mathbf{z}_1$ is better than $\mathbf{z}_2$ in all objectives	$Z_1 \succ\succ Z_2$	Every solution in Z_2 is strictly dominated by at least one solution in Z_1
Dominates	$\mathbf{z}_1 \succ \mathbf{z}_2$	$\mathbf{z}_1$ is better than $\mathbf{z}_2$ in at least one objective and is not worse in any objective	$Z_1 \succ Z_2$	Every solution in Z_2 is dominated by at least one solution in Z_1
Better			$Z_1 \rhd Z_2$	Every solution in Z_2 is weakly dominated by at least one solution in Z_1 and $Z_1 \neq Z_2$
Weakly dominates	$\mathbf{z}_1 \succeq \mathbf{z}_2$	$\mathbf{z}_1$ is at least as good as $\mathbf{z}_2$ in all objectives	$Z_1 \succeq Z_2$	Every solution in Z_2 is weakly dominated by at least one solution in Z_1
Incomparable	$\mathbf{z}_1 \| \mathbf{z}_2$	Neither $\mathbf{z}_1$ nor $\mathbf{z}_2$ weakly dominates the other	$Z_1 \| Z_2$	Neither Z_1 nor Z_2 weakly dominates the other

Table C.1: Definitions of dominance relationships between solutions and between frontiers, reproduced from Zitzler *et al.* [72].

C.1.1 *Additive binary epsilon indicator* $I_{\epsilon_+ 2}$

Given two frontiers, Z_1 and Z_2, the additive binary epsilon indicator is defined as [72]

$$I_{\epsilon_+ 2}(Z_1, Z_2) = \inf_{\epsilon \in \mathbb{R}} \{ \forall \mathbf{z}_2 \in Z_2 \; \exists \mathbf{z}_1 \in Z_1 : \mathbf{z}_1 \succeq_{\epsilon_+} \mathbf{z}_2 \} \tag{C.3}$$

where $\succeq_{\epsilon_+}$ is the additive ϵ-dominance relationship:

$$\mathbf{z}_1 \succeq_{\epsilon_+} \mathbf{z}_2 \iff \epsilon + \mathbf{z}_1^i \geq \mathbf{z}_2^i \quad \forall 1 \leq i \leq N \tag{C.4}$$

Intuitively, ϵ is the minimum amount by which a frontier Z_1 must be translated such that every solution $\mathbf{z}_2 \in Z_2$ is "covered". See Figure C.1. Positive values of $I_{\epsilon_+ 2}(Z_1, Z_2)$ indicate the presence of points $\mathbf{z}_2 \in Z_2$ that are not dominated by Z_1. Negative values of $I_{\epsilon_+ 2}(Z_1, Z_2)$ indicate that Z_1 strictly dominates Z_2 ($Z_1 \succ\succ Z_2$).

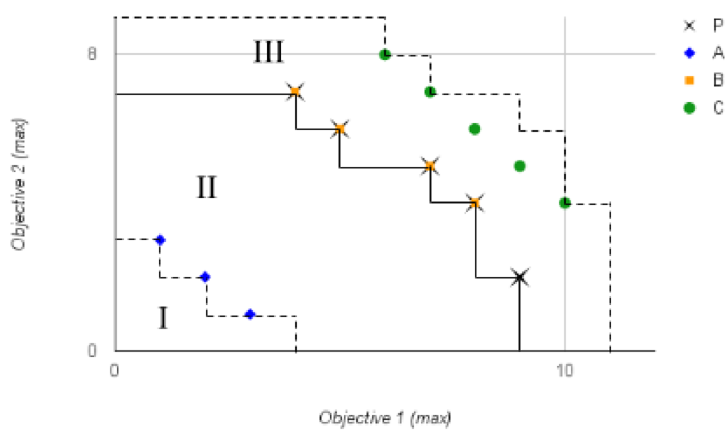

Figure C.1: Depiction of the additive binary epsilon indicator $I_{\epsilon_+ 2}$ and the additive epsilon dominance relationship $\succeq_{\epsilon_+}$. In the figure,

$$I_{\epsilon_+ 2}(P, A) = -4 < 0 \qquad I_{\epsilon_+ 2}(P, B) = 0 \qquad I_{\epsilon_+ 2}(P, C) = 2 > 0$$

Region III is ϵ_+-dominated for $\epsilon = 2$; region II is ϵ_+-dominated for $\epsilon = 0$; region I is ϵ_+-dominated for $\epsilon = -4$. Note that region II also encompasses region I, and region III encompasses region II.

C.1.2 Additive unary epsilon indicator I_{ϵ_+}

I define the unary epsilon indicator as

$$I_{\epsilon_+}(Z) = I_{\epsilon_+2}(Z, \mathbf{z}_{\text{ideal}}) \tag{C.5}$$

That is, the additive unary epsilon indicator is identical to the additive binary epsilon indicator where the second frontier consists of a single point: the ideal solution for the first frontier.

This differs from the unary epsilon indicator traditionally used in EMO [72]. In EMO, the frontier is compared against a reference nondominated set. However, because the frontiers in the present study have guaranteed optimality, there is no reference set against which to compare them.

C.1.3 Unary hypervolume indicator I_{H1} and binary hypervolume indicator I_{H2}

For every solution $\mathbf{z}_i$ in a frontier Z define the hyperrectangle r_i whose diagonal corners are the origin and the objective vector $\mathbf{z}_i = \langle z^1, \ldots, z^N \rangle$ (see Figure C.2). Then the unary hypervolume indicator of the frontier Z is the N-dimensional volume of the union of all of the hyperrectangles corresponding to the solutions in Z:

$$I_{H1}(Z) = \text{vol}\left(\bigcup_{i=1}^{|Z|} r_i \right) \tag{C.6}$$

Then define the binary hypervolume indicator of two frontiers Z_1 and Z_2 as [71]

$$I_{H2}(Z_1, Z_2) = I_{H1}(Z_1 + Z_2) - I_{H1}(Z_2) \tag{C.7}$$

where $I_{H1}(Z_1 + Z_2)$ is the unary hypervolume indicator of the frontier consisting of the nondominated points in $Z = \{z \in Z_1 \cup Z_2\}$. See Figure C.3. The binary hypervolume indicator provides the volume of frontier Z_1 that is not contained within frontier Z_2. Larger values of I_{H1} correspond to frontiers occupying larger amounts of the objective space. In a

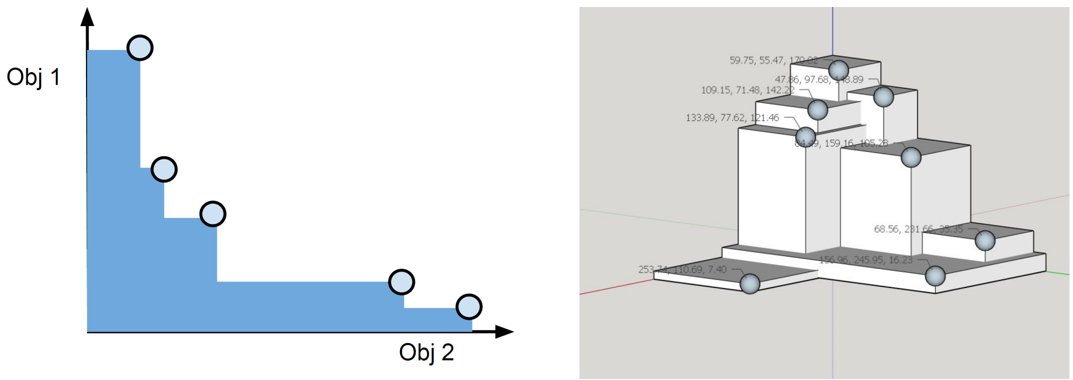

Figure C.2: Depiction of the hypervolumes of frontiers with two objectives (left) and three objectives (right).

normalized objective space, $I_{H2}(Z_1, Z_2) > I_{H2}(Z_2, Z_1)$ indicates areas of less conflict between objectives in Z_1 than in Z_2.

I developed a custom algorithm to solve for the hypervolume idicators. The details of the algorithm may be found in §A.

C.1.4 Unary distance indicator I_d

The unary distance indicator measures the average distance from the frontier to the ideal solution:

$$I_d = \frac{\sum_{\mathbf{z}\in Z} ||\mathbf{z}_{\text{ideal}} - \mathbf{z}||}{N} \tag{C.8}$$

Smaller values of I_d correspond to frontiers that are closer to the ideal solution, which may imply less conflict between objectives. This metric is analogous to the unary distance indicator more commonly used in EMO [17]. Where the metric used here measures the distance to the ideal solution, the traditional metric measures the distance to a reference Pareto frontier.

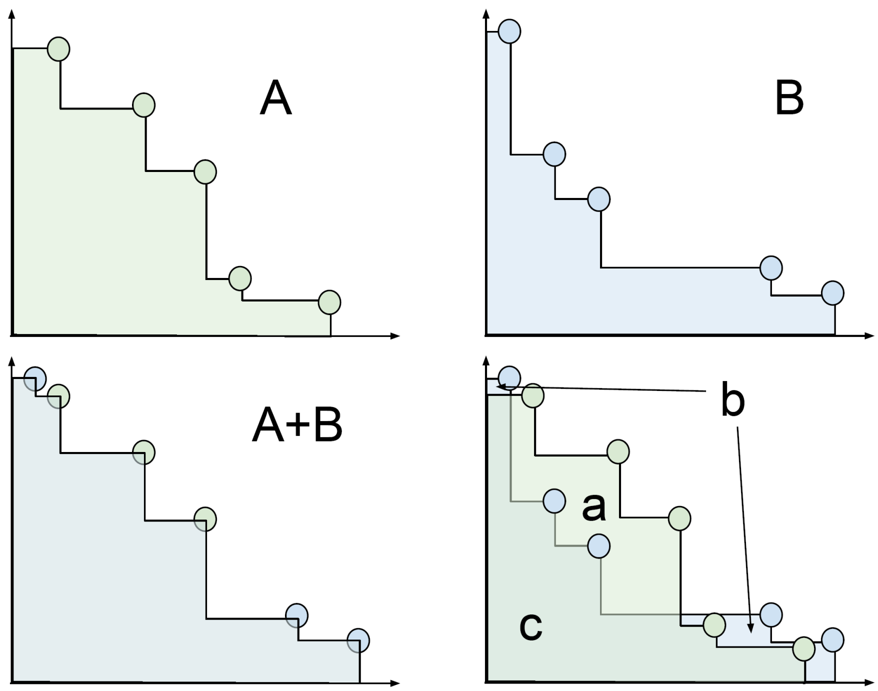

Figure C.3: Depiction of the binary hypervolume indicator. The individual frontiers are shown in the top row: frontier A (left) and frontier B (right). The merged frontier $A + B$ is shown in bottom left - note the absence of points that were dominated when combined. Following the naming of regions as shown in the bottom right figure, the binary hypervolume indicator is equal to

$$I_{H2}(A, B) = (\text{area}_a + \text{area}_b + \text{area}_c) - (\text{area}_b + \text{area}_c) = \text{area}_a$$

C.1.5 Unary Spacing Indicator I_s

The unary spacing indicator, or Schott's spacing metric [55], computes the standard deviation of the distance between points in the frontier:

$$I_s = \sqrt{\frac{1}{N-1} \sum_{\mathbf{z} \in Z} (d_z - \bar{d})^2} \tag{C.9}$$

where

$$d_z = \min_{\mathbf{y} \in Z, \mathbf{y} \neq \mathbf{z}} ||\mathbf{z} - \mathbf{y}|| \tag{C.10}$$

and $\bar{d}$ is the average over all d_z. In EMO, the spacing indicator provides a measure of an algorithm's ability to search the frontier space uniformly. Here, the spacing metric provides a measure of the flexibility afforded to the decision maker under each climate scenario, since smaller values of I_s imply a higher density of solutions and greater flexibility.

C.2 Intra-Frontier Comparison Metrics

While the above methods provide frontier-level metrics of conflict and tradeoffs, there are two methods employed here to also determine the degree of conflict within a single frontier. The first is an approach used in many-objective optimization, and the second is a variant of the unary hypervolume indicator.

C.2.1 Pearson correlation coefficients

Given the increased difficulty in solving many-objective optimization problems [38], researchers in this field seek to reduce the number of objectives considered in the model. To determine which objectives most strongly influence the shape of the frontier, they compute the correlation between each pair of objectives [20]. Objective pairs with strong negative correlation conflict with one another. The Pearson correlation coefficients are computed per

$$\rho_{X,Y} = \frac{\mathrm{cov}(X,Y)}{\sigma(X)\sigma(Y)} \tag{C.11}$$

where, for objectives x and y, X and Y are

$$X = \{\mathbf{z}_1^x, \mathbf{z}_2^x, \ldots, \mathbf{z}_{|Z|}^x\} \tag{C.12}$$

$$Y = \{\mathbf{z}_1^y, \mathbf{z}_2^y, \ldots, \mathbf{z}_{|Z|}^y\} \tag{C.13}$$

C.2.2 Area of 2D frontier projection A_{xy}

The second intra-frontier comparison metric uses the unary hypervolume indicator described in §C.1.3. Given a frontier with objective vectors in N dimensions, take two objectives x and y, and project the N-dimensional frontier to the two-dimensional xy-plane. Remove solutions dominated in this projection, and compute the hypervolume indicator (which, in two-dimensions, is simply the area). See Figure C.4. Larger values of A_{xy} imply less conflict between objectives x and y.

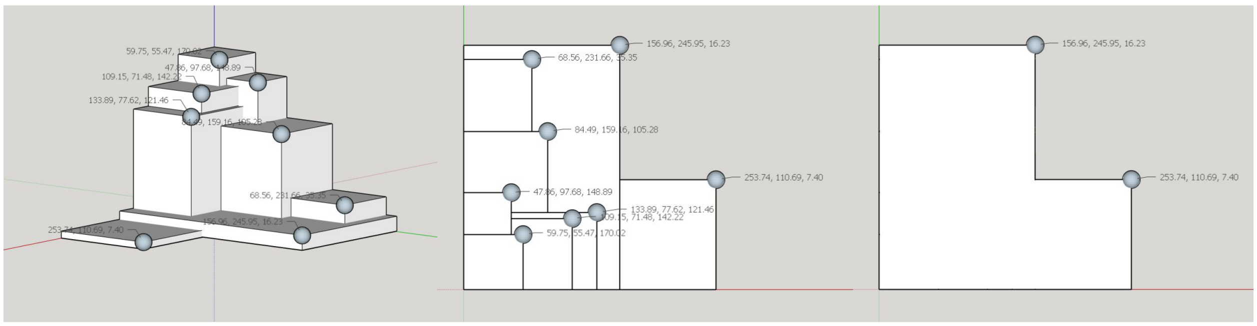

Figure C.4: Comparing conflict between objectives based on the area bounded by two-dimensional frontier projection. Left is the original frontier; middle shows the 2D projection of the frontier; right shows the projected frontier with all dominated solutions removed. Assuming both objectives are maximized, the larger the area bounded by the cross-sectional area, the less conflict between the objectives.